Electrocaloric Cooling

Gunnar Suchaneck, Oleg Pakhomov and
Gerald Gerlach

Abstract

The *electrocaloric effect* describes a reversible temperature change in dielectric materials submitted to an applied electric field. Adiabatic polarization raises their temperature, and adiabatic depolarization lowers it, analogous to temperature changes that occur when a gas is compressed or expanded. For refrigerator application, the reverse Brayton cycle is currently the most promising for practical implementation. The electrocaloric effect provides a large material efficiency. However, existing refrigerator prototypes lack from the absence of efficient heat switches for thermal linkage to the load and the heat sink. Cooling power densities of a few W/cm^2 and temperature spans in the order of 20 K (in regeneration systems) are achievable at a cycle time of 100 ms.

Keywords: electrocaloric effect, thermodynamic cycles, coefficient of performance, refrigeration devices

1. Introduction

For almost 150 years, refrigeration applications were solved by means of vapour compression. While the most efficient fluids for this approach are based on chlorofluorocarbons, hydrochlorofluorocarbons and hydrofluorocarbons, they come with the severe drawback of contributing to global warming and ozone depletion. Therefore, in 1987, the Montreal Protocol issued a ban on these chemicals providing regulations for phasing them out. Promising natural alternative substances are impractical due to their toxicity (ammonia) or—in particular—their flammability (propane) [1].

Vapour compression refrigerators (VCRs) are operated as reverse Rankine cycles. They use a circulating liquid refrigerant as a medium. The refrigerant is: (i) adiabatically compressed, (ii) condensed at constant pressure undergoing a phase transition (thereby rejecting heat to the heat sink), (iii) adiabatically throttled in an expansion valve and (iv) evaporated at constant

pressure undergoing the reverse phase transition (thereby absorbing heat from the load). The amount of transferred heat is determined by the latent heat of the first-order phase transition. Similarly, in solid-state electrocaloric (EC) cooling, the adiabatic compression/expansion of the refrigerant is analogous to adiabatic polarization/depolarization, while the isobaric processes are replaced by isofield ones. Contrary to VCR, where the adiabatic expansion of the vapour is thermodynamically irreversible, the EC and the magnetocaloric (MC) effects are thermodynamically reversible processes that could reach the limit of the Carnot efficiency. This is another aspect making them promising for future application.

Electric fields required for the EC refrigeration cycle can be supplied much easier and less expensively than the high magnetic fields required for the MC refrigeration [2]. Other advantages in comparison with MC cooling are higher power densities due to potentially higher cycle frequencies, smaller mass of the device, compactness, potential cost reduction, independence on risks of rare-earth materials supply, etc. [3]. Moreover, electrical energy for EC cooling can be provided by stationary or mobile solar cells and by electric vehicle batteries. This opens up completely new possibilities for an environment-friendly industrialization of developing countries.

EC materials provide a solid-state cooling technology without polluting liquid refrigerants and no or almost absent moving parts (pump and motion of a pumped heat transfer fluid). Generally, EC material (refrigerant) converts the electrical input work

$$W = \int E dD, \tag{1}$$

into cooling or heating. Here, E is the electric field and D is the dielectric displacement. The latter is a vector field describing the electrical effect of free and bound charges in materials. Compared to VCR, the E plays the role of pressure and D plays the role of volume in vapour compression.

More detailed descriptions can be found in a number of recent reviews of the EC effect [2, 4, 5] and its application in refrigerators [3, 6, 7], and a book on this topic [8].

2. Electrocaloric effect

An electric field E applied to a dielectric material induces a change in dielectric displacement and, thus, a change in temperature and entropy in the material. The EC effect is a reversible temperature change of a material that results from an adiabatic application of an electric field. It was derived by Lord Kelvin based on the assumption of reversibility of the pyroelectric effect from thermodynamics in 1878 [9]: *If the preceding explanation of pyroelectricity be true, it must follow that a pyroelectric crystal moved about in an electric field will experience cooling effects or heating effects … in virtue of the wholly latent electric polarity of a seemingly neutral pyroelectric crystal (that is to say, a crystal at the surface of which there is an electrification neutralizing for external space the force due to its internal electric polarity), the same cooling and heating effects will be produced by moving it in an electric field, as similar motions would produce in a similar crystal which, by having been heated in hot water, dried at the high temperature, and cooled, is in a state of pyroelectric excitement.*

The first experimental investigations of the EC effect in Rochelle salt, KH_2PO_4, $BaTiO_3$ and $SrTiO_3$ date back to 1930 [10], 1950 [11], 1952 [12] and 1956 [13], respectively. However, the EC effect values reported since that time (at maximum 2.5 K in $Pb_{0.99}Nb_{0.02}(Zr_{0.75}Sn_{0.20}Ti_{0.05})O_3$ ceramics [14]) were too small for practical use.

EC cooling has regained attention in 2006, when Mischenko et al. could show that large electrical fields can be applied to antiferroelectric $PbZr_{0.95}Ti_{0.05}O_3$ thin films [15]. They observed that—close to the ferroelectric Curie temperature of 222°C—a field change from 77.6 to 29.5 V/μm induced an adiabatic temperature change of 12 K as it was determined from the integrated pyroelectric effect. Recently, another group showed that a lead-free stack of 63 $BaTiO_3$ thick films provides an EC temperature change of 7.1 K at an applied field of 80 V/μm [16]. The thickness of the individual layers deposited by tape casting and electrically contacted by inner Ni electrodes amounted to ca. 3 μm. In Ref. [17], commercially available multilayer capacitors (MLCs) even of 200 ceramic layers ($BaTiO_3$-based Y5V formulation) each 6.5 μm in thickness were used as a refrigerant [17]. Here, an EC temperature change of 0.5 K was obtained at 30 V/μm. The MLC concept was developed by Herbert [18] and introduced in the early 1980s by Murata Manufacturing Co. for the fabrication of base metal monolithic capacitors [19]. MLCs are now in mass production (some 5×10^{11} pieces per year) by means of sheeting green ceramic tapes and screen-printing technology [20]. However, they are not optimized for EC applications. Commercial EC devices are still not available.

EC devices are driven by an electric field strength. That means that a voltage has to be applied. In this case, the independent thermodynamic parameters are temperature T and electric field E. According to the second law of thermodynamics, an infinitesimal amount of heat dQ transferred into the system by an entropy change dS is then given by

$$dQ = TdS = T\left[\left(\frac{\partial S(E,T)}{\partial T}\right)_E dT + \left(\frac{\partial S(E,T)}{\partial E}\right)_T dE\right], \quad (2)$$

where S is the entropy per unit volume. Following the definition of volumetric specific heat at constant E, c_E, the first term in parentheses can be replaced by

$$\left(\frac{\partial S(E,T)}{\partial T}\right)_E = \frac{c_E(E,T)}{T}. \quad (3)$$

The value of $c_E(E,T)$ is usually represented by the zero-field value in the temperature range of interest $c = c(T)$. With regard to Maxwell's equations, entropy S and dielectric displacement D are coupled [21]

$$\left(\frac{\partial S}{\partial E}\right)_T = \left(\frac{\partial D}{\partial T}\right)_E = \pi_E, \quad (4)$$

where π_E is the pyroelectric coefficient at constant electric field. Considering now a ferroelectric material exhibiting below T_C a remnant polarization P_r and an induced polarization $\varepsilon\varepsilon_0 E$, and a dielectric displacement of

$$D(T, E) = \varepsilon_0\varepsilon(T, E)E + P_r(T), \tag{5}$$

Eq. (2) takes the form:

$$dQ = c_E dT + T\left(\frac{\partial P_r(T)}{\partial T} + \varepsilon_0 E \frac{\partial \varepsilon(T, E)}{\partial T}\right)_E dE. \tag{6}$$

Thus, the EC temperature change is given by two terms [22]:

$$\Delta T_{EC} = -\frac{T}{c_E}\int_{E_1}^{E_2}\left(\frac{\partial P_r(T)}{\partial T} + \varepsilon_0 E \frac{\partial \varepsilon(T, E)}{\partial T}\right)_E dE. \tag{7}$$

In the ferroelectric phase, below T_C, the contributions of spontaneous and induced polarization partially compensate each other, because in this temperature region the temperature coefficients behave oppositely: $\partial\varepsilon/\partial T > 0$ and $\partial P_r/\partial T < 0$. In $SrTiO_3$ ceramics below the temperature of maximum dielectric permittivity, in antiferroelectrics with $\langle P_r \rangle = 0$, and in some relaxors with $\partial Pr/\partial T > 0$, a negative electrocaloric effect can be obtained below T_C, that is, the sample is cooled during adiabatic electric field application.

Figure 1 compares the ΔT_{EC} values of $BaTiO_3$ above T_C ($P_r{\rightarrow}0$) calculated from Eq. (7) [23] with available experimental data [12, 16, 24, 25]. Well-known examples of EC materials driven above the temperature of maximum dielectric permittivity are polyvinylidene fluoride terpolymers and irradiated copolymers, both exhibiting relaxor behaviour. Here, assuming a dielectric permittivity
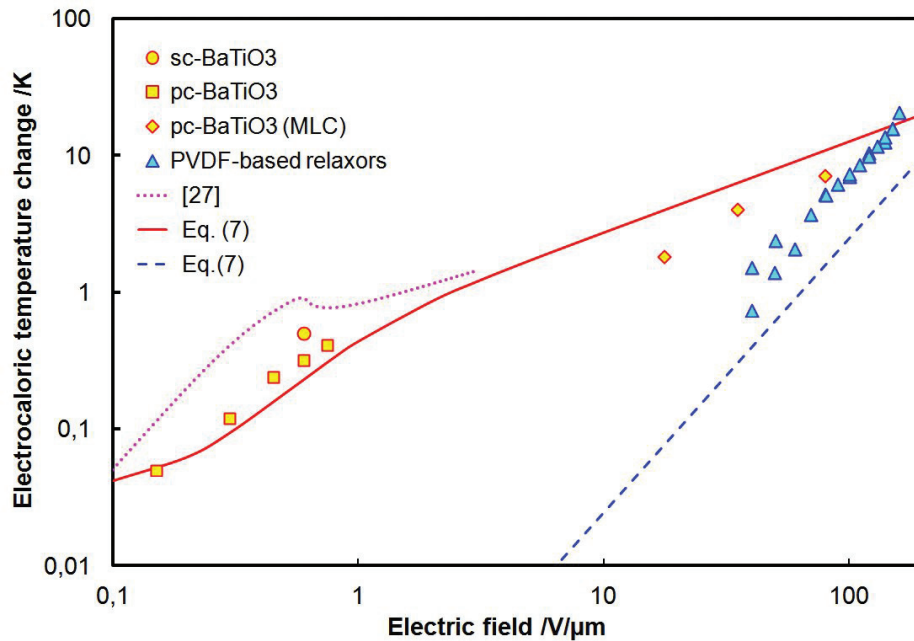
Figure 1. ΔT_{EC} of $BaTiO_3$ [23] (solid line) and PVDF-based relaxor polymers (dashed line) as a function of E calculated for $P_r = 0$ following Eq. (7) in comparison to ΔT_{EC} determined along the coexistence curve of the ferroelectric-paraelectric phase transition [27]. Experimental data of single crystal (sc), polycrystalline (pc) $BaTiO_3$, and PVDF-based polymers were taken from Refs. [12, 16, 24, 25, 28], respectively.

independent on electric field, our calculations revealed that suitable for application ΔT_{EC} values appears only at large electric fields. This is a problem since rapidly rising electric fields favour electrical breakdown of polymers. Moreover, the field dependence of ΔT_{EC} is very different to BaTiO$_3$, but similar to relaxor PLZT in Ref. [26].

In the presence of a first-order phase transition induced by an electric field $E_{PT} < E_2$, an additional entropy ΔS_{PT} change occurs at the phase transition temperature T_{PT} which is originated from the latent heat L

$$\Delta S_{PT} = \frac{L}{T_{PT}}.$$ (8)

Along the coexistence curve between two phases of the considered constituent, E is no longer an independent parameter. Therefore, it should be substituted by D. The slope of the coexistence curve on the E-T diagram is then given by the Clapeyron equation [29]

$$\frac{dE_{PT}}{dT} = \frac{\Delta S_{PT}}{\Delta T} = \frac{L}{T\Delta D}.$$ (9)

In the case of ferroelectrics, where dielectric displacement D approximately equals the polarization P, this yields a ΔT_{EC} of [4]

$$\Delta T_{EC,PT} = \frac{T}{c_p} \cdot \frac{dE_{PT}}{dT} \cdot \Delta P,$$ (10)

where ΔP is the jump of polarization at the phase transition, and c_P is the volumetric-specific heat at constant P. **Table 1** lists the Clausius-Clapeyron contribution to the EC effect of some typical ferroelectrics.

The EC effect of a first-order phase transition increases along the coexistence curve up to the tricritical point. With further increase of the applied field, it decreases it again [27]. Thus, the Clausius-Clapeyron contribution is substantial only for bulk ceramic-based EC devices driven at moderate electric fields.

Considering the entropy change $\Delta S = S(0, T) - S(E, T)$ for a system of N dipolar entities, each having Ω discrete equilibrium orientations, a physical upper bound on the EC effect was derived in Ref. [35]:

$$\Delta T_{EC,max} = \frac{T \cdot ln\Omega}{3\varepsilon_0 \cdot c \cdot C_{CW}} P_s^2,$$ (11)

where C_{CW} is the Curie-Weiss constant and P_s the polarization at saturation when all dipoles are aligned along the field. Values of P_s might be obtained from hysteresis loops in the saturation regime. Values of C_{CW} can be derived from the asymptotic behaviour of the linear dielectric susceptibility in a Curie-Weiss-plot $\varepsilon \propto C/(T - T_0)$ with $T_0 < T_C$. T_0 is the Curie-Weiss temperature, i.e. the temperature of the appearance of a metastable paraelectric phase in the ferroelectric one. The upper limit $\Delta T_{EC,max}$ of lead-based relaxors estimated in this manner

Composition	T_{PT}, °C	$\Delta T_{EC,PT}$, °C	Ref.
PbTiO$_3$	493	10	[4]
KNbO$_3$	435	6	[4]
PbZrO$_3$	230	13	[4]
Pb(Zr$_{0.95}$Ti$_{0.05}$)O$_3$	230	12	[4]
Pb$_{0.99}$Nb$_{0.02}$(Zr$_{0.75}$Sn$_{0.20}$Ti$_{0.05}$)O$_3$	163	3.0	[4]
[111] 0.705PbMg$_{1/3}$Nb$_{2/3}$O$_3$-0.295PbTiO$_3$	127	0.55	[4]
BaTiO$_3$	120	1.5	[4]
P(VDF-TrFE)68/32	~105	~12	[30] (Suppl.)
P(VDF-TrFE)65/45	81	9.5	[8], p.112
P(VDF-TrFE)55/45	~65	~4[1]	[30] (Suppl.)
0.87PbMg$_{1/3}$Nb$_{2/3}$O$_3$-0.13PbTiO$_3$	18	0.2	[31]
0.9PbMg$_{1/3}$Nb$_{2/3}$O$_3$-0.1PbTiO$_3$	5	0.8	[32, 33]
PbSc$_{0.5}$Ta$_{0.5}$O$_3$	2	1.6	[4]
0.95PbMg$_{1/3}$Nb$_{2/3}$O$_3$-0.05PbTiO$_3$	−28	0.13	[33, 34]
[111] PbMg$_{1/3}$Nb$_{2/3}$O$_3$	−55	0.33	[34]
NH$_4$H$_2$PO$_4$	−123	8.2	[4]
KH$_2$PO$_4$	−153	0.7	[4]

[1]Calculated using Eq. (12).

Table 1. EC temperature change corresponding to the latent heat calculated using Eqs. (9) or (10) from experimental values.

amounts to about 10 K. The EC temperature of a first- or second-order phase transition deduced from the specific heat curves yields:

$$\Delta T_{EC} = \int_{T_1}^{T_2} \left[\frac{c_p(T)}{c_p^{ph}(T)} - 1 \right] dT, \tag{12}$$

where c_p^{ph} is the portion of volumetric-specific heat at constant pressure p due to lattice vibrations. For a second-order phase transition in PZT thin films, ΔT_{EC} amounts to 4.0–5.3 K at 665 K [36]. A phase-transition independent upper bound of the EC effect was proposed in Ref. [37] based on the fact that only a certain energy density might be stored in a dielectric—equivalent to a limit in electrostatic pressure. Electrical breakdown of metal oxide dielectrics is fixed by the arising local electric field and the chemical bond strength leading to $E_{max} \propto \varepsilon^{-1/2}$, with E_{max} the dielectric strength of the EC material [38]. According to Eq. (7), this results for $P_r \to 0$ in:

$$\Delta T_{EC,max} < -\frac{\varepsilon_0 T}{2c} \cdot \frac{1}{\varepsilon(0,T)} \frac{\partial \varepsilon(0,T)}{\partial T} \cdot \varepsilon(0,T) E_{max}^2. \tag{13}$$

For a relaxor ferroelectrics exhibiting a huge temperature dependence of dielectric permittivity $\frac{1}{\varepsilon(0,T)} \frac{\partial \varepsilon(0,T)}{\partial T} \approx 10^{-2} \text{K}^{-1}$ [39], we estimate an ultimate EC temperature change of $\Delta T_{EC,max} \approx 50\text{K}$.

Our estimation explains the high values of the EC effect previously obtained in relaxor lead-lanthanum zirconate-titanate thin films [26].

3. Thermodynamic cycles

3.1. Carnot cycle

An EC refrigerator working under the Carnot cycle will reach the highest efficiency possible. The Carnot cycle describes a reversible change of an ideal gas, which allows to convert a given amount of thermal energy into work, or, conversely, to provide cooling using a given amount of work. It consists of four steps of operation: two adiabatic and two isothermal ones. During the adiabatic steps, no heat is transferred while the refrigerant absorbs heat from the load at its minimum temperature and expels heat to the heat sink at its maximum temperature in the isothermal steps.

The EC Carnot cycle is demonstrated in **Figure 2**. The cycle starts from point 1 where the electric field on the EC material is E_1. In steps 1–2, the electric field is increased adiabatically to E_3. Here, the entropy of the EC material stays constant, and therefore, the temperature increases. At point 2, the EC material starts to experience an isothermal process. The electric field will be increased until it reaches its maximum value E_4 at point 3. In order to conserve isothermal conditions, heat should be simultaneously rejected to the heat sink. In the adiabatic steps 3–4, the electric field is decreased to E_2 while the temperature of the EC material decreases until reaching point 4. In the second isothermal steps 4–1, the electric field decreases to E_1 while heat should be absorbed from the load. Thus, the Carnot cycle requires a minimum of four different electric fields. Since the heat rejected to the heat sink amounts to $Q = T_1 \Delta S$, the cooling power depends significantly on the chosen working point (cf. cycles 1-2-3-4 and 5-6-7-8).
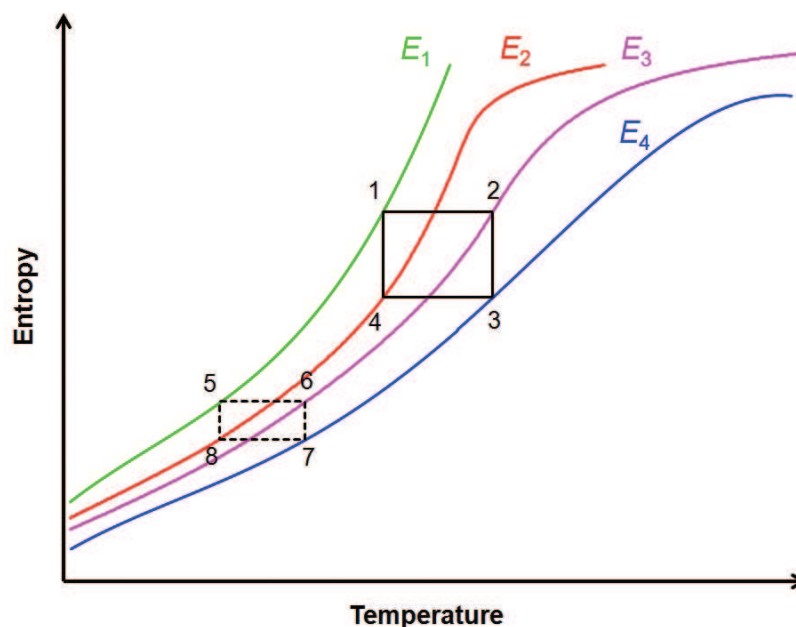

Figure 2. Reverse Carnot cycle for EC refrigeration.

The implementation of the Carnot cycle into a practical refrigeration system is challenging, since the isothermal steps and the transition from an adiabatic process to an isothermal one are not easy to realize. In the two isothermal steps, the refrigerant is in thermal contact with the load or the heat sink, respectively. Here, the rate of electrical field change is limited by the relatively large thermal relaxation time of the thermal interfaces (heat switch or heat transfer agent) of the system. This significantly lowers cycle time. Moreover, the maximum temperature span $T_{span} = T_l - T_s$ of the whole refrigerator will be less than the ΔT_{EC} of the EC material. On the one hand, a small temperature span provides large cycle efficiency (cf. Eq. (14)). The temperature span $T_l - T_s$ might be increased by means of a cascaded structure of m units where the unit n ejects heat to unit $n + 1$, while this unit absorbs heat from unit n ($1 < n < m$) covering the desired $T_l - T_s$. Such a cascade system does not require large ΔT_{EC}. However, in order to reach high efficiency, the heat ejected from the previous step should be completely absorbed by the following step. In general, since the EC-induced entropy change is not a constant, and the specific heat of the EC material also changes with temperature, this requirement is hard to meet. Consequently, the performance of the cascaded refrigerator is further reduced.

The coefficient of performance COP is defined as the ratio between the useful heating or cooling provided to work required. Considering an ideal Carnot cycle, the corresponding COP_C can be written as

$$COP_C = \frac{T_s}{T_l - T_s},\tag{14}$$

where T_s and T_l indicate the temperature of heat sink and load, respectively. COP_C establishes an upper bound for the COP. Since the EC effect is a thermodynamically reversible process, EC refrigerators could reach the limit of the Carnot efficiency. The relative efficiency of a refrigerator with respect to an ideal Carnot cycle is defined as

$$\Phi = \frac{COP}{COP_C},\tag{15}$$

where Φ is determined by the EC material hysteresis, the heat losses of the heat transfer processes through heat switches or a regenerator, the thermal resistance of the heat switches, the regenerator efficiency (the ratio of actual heat exchange in the regenerator to an ideal one), the heat flow from the environment to the load, the deviation of the isothermal steps from the ideal case, Joule heating at the contacts, etc. The total efficiency is then the product of separate efficiency coefficients. The current state-of-the-art commercial vapour compression cycle has a COP of about 3.6 [7].

3.2. Alternative refrigeration cycles

Similar to MC cooling, also alternative refrigeration cycles might be employed for EC refrigeration. The Stirling and Ericsson cycles were considered in Ref. [40]. The Stirling refrigeration cycle consists of two isothermal and two isopolarization steps, while the Ericsson refrigeration cycle consists of two isothermal and two isofield steps. The heat is released and absorbed in the two

isothermal steps. In the Stirling cycle, polarization would change during heating and cooling due to a strong temperature dependence of the dielectric permittivity of polar dielectrics. Therefore, this cycle is not suitable for EC refrigeration from an experimental point of view. The Ericsson cycle is more readily applicable than other thermodynamic cycles such as the Stirling cycle. An isofield condition is easily realized keeping the EC material connected to the voltage source. The Ericsson cycle requires heat regeneration, i.e. the heat rejected from the hot refrigerant is intermittently stored in a thermal transfer medium, before it is transferred to the cool refrigerant. The efficiency of the regenerator is significantly affected by the heat transfer conditions (heat transfer surface, heat transfer coefficient, boundary layers, heat conduction, fluid viscosity, etc.). Generally, the coefficient of performance of a ferroelectric Ericsson refrigeration cycle is smaller than that of a Carnot cycle for the same temperature range [40].

The Olsen cycles was proposed for application in pyroelectric energy harvesting [41]. Therefore, it will not be considered in this work. It replaces adiabatic polarization and depolarization of a ferroelectric by corresponding isothermal steps.

A gas refrigeration cycle where a gas is compressed and expanded, but does not change phase, is called Bell-Coleman cycle. It consists of two adiabatic (compression and expansion) and two isobaric processes (heat addition and heat rejection). This cycle corresponds also to the reverse Brayton cycle widely used for subcooling in the liquid nitrogen industry. For EC refrigerators, even the reverse Brayton cycle is predominantly chosen [42–44]. It includes the following steps (**Figure 3**):

1. Adiabatic polarization by increasing the electric field to a value E_2, the EC material experiences EC heating ($+\Delta T_{EC}$).
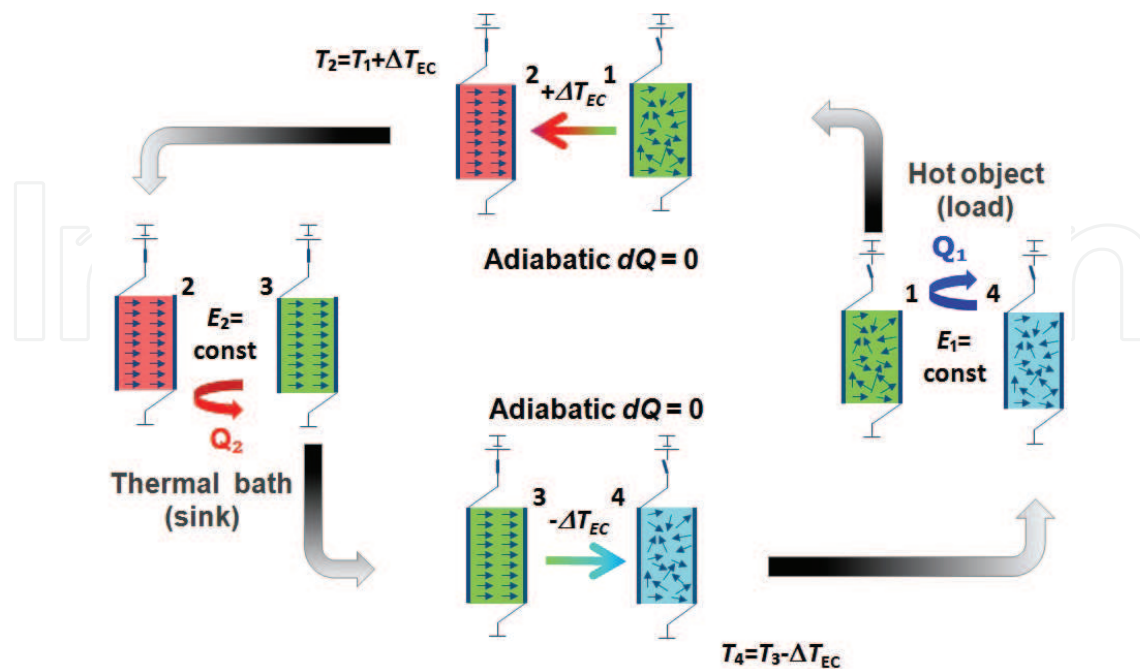

Figure 3. Reverse Brayton cycle for EC refrigeration.

2. Heat rejection: heat rejection to a heat sink under a constant electric field E_2.

3. Adiabatic depolarization by decreasing the electric field to a value E_1, e.g. zero, the material experiences EC cooling by $(-\Delta T_{EC})$.

4. Heat absorption from a load under the constant electric field E_1 returning to the initial state.

The amount of heat transferred from the load to the heat sink per cycle and per unit volume is given by

$$q = c(E_2) \cdot (T_2 - T_3), \tag{16}$$

where $c(E_2)$ is the volumetric-specific heat at $E = E_2$. The cooling power is then $\langle \dot{q} \rangle = q/\tau_c$ with τ_c the cycle time. The difference between the Brayton and Ericsson cycles is that the Brayton cycle uses adiabatic steps instead of using isothermal ones. Compared to the Carnot cycle, the mean temperature during heat rejection to the heat sink will be less than T_2, whereas the mean temperature during heat absorption from the load is higher than T_4. For an ideal gas and a specific heat independent on temperature, the relative refrigerator efficiency amounts to $\Phi \approx 1/4$ [45]. Ferroelectrics themselves exhibit a strong temperature dependence of the volumetric-specific heat, particularly in the vicinity of the ferroelectric-paraelectric phase transition. The relative refrigerator efficiency then comes out as

$$\Phi = \frac{c(E_2)(T_3 - T_2)}{c(E_1)(T_4 - T_1) - c(E_2)(T_3 - T_2)}. \tag{17}$$

This means that it is determined by the ratio $c(E_1)/c(E_2) > 1$. Consequently, it leads to $\Phi < 0.25$. Here, Φ is also largely affected also by the ratio of T_{span} to ΔT_{EC}, i.e. $(T_2 + T_3)/2 \sim \Delta T_{EC}$, which are functions of the EC material, the EC element design and the thermal interfaces. However, this estimation does not account for the losses described in detail below. With regard to losses, Φ is limited to a value of approximately 10–15%, which is comparable to thermoelectric energy converters. Efficiencies of $\Phi \geq 0.5$ have been reported in literature for a micro-EC cooling module comprising a micro-electromechanical heat switch [46], a chip scale EC oscillatory refrigerator (ECOR) [28] and a EC refrigerator with intrinsic regenerator [47]. It seems that such a Φ value originates from unreasonably large values of $COP > 8$.

Considering only heat losses caused by heat switches, the maximum relative efficiency of EC refrigerators is given by [48]

$$\Phi_{switch} = \left(\frac{\sqrt{K} - 1}{\sqrt{K} + 1} \right)^2, \tag{18}$$

where $K = \kappa_{on}/\kappa_{off}$ is the conductivity contrast of the heat switches and, κ_{on} and κ_{off} are the thermal conductivities of the heat switch in the on and off states, respectively. Thus, if $K > 10$, then EC cooling exceeds the efficiency of thermoelectric cooling. For $K > 100$, it offers an

efficiency comparable to magnetic cooling (about 70%) with much smaller and cheaper equipment. With regard to the thermal conductivity of the EC element κ_{EC} [23], the thermal contrast is

$$K' = K \cdot \frac{\kappa_{off} + \kappa_{EC}}{\kappa_{on} + \kappa_{EC}}. \tag{19}$$

For applications, usually $\kappa_{EC} \approx \kappa_{on} \gg \kappa_{off}$ holds.

To cyclically store and release energy to the refrigerant, cyclic operating EC systems require a regenerator. In vapour compression refrigeration, the refrigerant is also the circulating fluid. Similarly, an EC material is used as both the refrigerant and the regenerator. However, an exchange fluid is needed to transport heat to and from the refrigerant since the refrigerant is a solid. Such an active EC regenerator (AER) consists of a porous structure of an EC material and voids or channels through which the heat transfer fluid can flow [42]. Regenerators are also a source of heat loss [40].

4. Optimal EC materials and optimal operational parameters

4.1. EC figure of merit

One way to characterize the performance of devices is the derivation of appropriate figures of merits *FOM*, that is, of appropriate combinations of physical properties affecting device efficiency. The EC device performance is determined by (i) the performance of the refrigeration cycle, (ii) the refrigeration capacity (*RC*) and (iii) the heat transfer efficiency. The different design of EC refrigerators makes a general treatment difficult. Therefore, we will consider first a *FOM* of cooling power based on materials performance instead of system performance. Our *FOM* accounts only for the thermal resistance at the interfaces of the EC material. It does not take into account the thermal mass of the heat switch or the heat transfer agent. Moreover, we assume that the heat transfer does not limit device efficiency, i.e. in case of a heat switch the thermal contrast becomes infinite: $K \rightarrow \infty$ (cf. Eq. (18)). We denote this model as an ideal EC element.

In order to characterize the maximum potential of the refrigerant for each cooling technology, an energy conversion efficiency originating from the material, COP_{mat}, was derived in Ref. [7]. It does not include the system details such as limitations in the driving system efficiency (from compressor, motor, etc.), system dynamics, regenerator effectiveness, heat or mass transfer and component geometries. Therefore, it can be regarded as the maximum potential the material has for the cooling technology. In the case of EC cooling, COP_{mat} yields [7]:

$$COP_{mat, EC} = \frac{T_s \Delta S - A_{EC}}{(T_l - T_s)\Delta S + 2A_{EC}}, \tag{20}$$

where A_{EC} is a materials constant appearing for hysteresis and dielectric losses. In Eq. (20), $T_s \Delta S$ represents the heat transferred from the load to the heat sink within one refrigeration cycle and $(T_l - T_s)\Delta S$ the work supplied by the EC material within this cycle. For $A_{EC} \rightarrow 0$,

Eq. (20) turns into Eq. (14) describing a thermodynamically reversible process. The COP_{mat} of EC materials (~0.35) is inferior to the ones of MC (~0.86) and elastocaloric materials (~0.65) which both exhibit a much larger latent heat of the corresponding first-order phase transitions [7]. Actually, EC refrigerators benefit much less from the large entropy change induced by driving the material through the phase transition by means of applying of releasing relatively small fields (cf. **Table 1**).

Eq. (20) includes a device-related parameter—the temperature span $(T_l - T_s)$, a thermodynamic parameter ΔS and a physical parameter A_{EC}. For practical use, it would be extremely helpful to implement a refrigerant materials criterion which characterizes the efficiency of the physical cooling process and which is therefore independent on the performance of different thermodynamic cycles. For this purpose, COP_{mat} may be written as [7]

$$COP_{mat} = COP_C \cdot \Phi_{mat}. \tag{21}$$

where Φ_{mat} is the dimensionless material efficiency:

$$\Phi_{mat} = 1 - \frac{\varepsilon\varepsilon_0 E^2 \cdot tan\delta}{c\Delta T_{EC}}, \tag{22}$$

where $tan\delta$ is the sum of dielectric and hysteresis losses during E cycling. The temperature difference $\Delta T* = \Delta T_{EC} - (T_l - T_s)$ of the heat transfer steps was replaced by its maximum value ΔT_{EC} since we consider the maximum cooling power (cf. Eq. (26)). Then Φ_{mat} becomes independent on cycle parameters, and it receives its minimum value. The second term on the right-hand side of Eq. (22) represents the inverse of the EC efficiency, i.e. the ratio between the heat transferred from the load to the heat sink and the dissipated electrical energy, introduced in Ref. [49].

The RC is a measure of how much heat can be transferred between the load and the heat sink in one ideal refrigeration cycle [50]:

$$RC = \int_{T_1}^{T_2} \Delta S dT \approx \Delta S \cdot \delta T = \frac{c\Delta T_{EC}}{T}\delta T, \tag{23}$$

where δT is the full width at half maximum of the ΔS versus T curve. Estimations of δT for different EC materials were given in Ref. [51]. Another physical estimate is the distribution width of the local Curie temperatures considered in Refs. [22, 37].

Complete heat transfer from and to the surroundings requires a Fourier number $Fo = \alpha t/d^2 > 1$, where α is the thermal diffusivity, t is the time and d is the thickness of the EC material [46]. Since power is the subject of interest, we have to consider the Fourier number per cycle time τ_c

$$\frac{Fo}{\tau_c} = \frac{\alpha}{d^2} = \frac{\kappa}{cd^2}, \tag{24}$$

with κ is the thermal conductivity. The FOM of an ideal EC element proposed in Ref. [37], combines the materials efficiency Φ_{mat}, the refrigeration capacity RC and the Fourier number per cycle time:

$$FOM = \frac{1}{1 - \Phi_{\text{mat}}} \cdot RC \cdot \frac{Fo}{\tau_c} = \frac{\kappa c \cdot \Delta T_{\text{EC.}}^2 \cdot \delta T}{\varepsilon \varepsilon_0 \cdot tan\delta} \cdot \frac{1}{T \cdot E^2 d^2} \cdot \tag{25}$$

This *FOM* consists of a term describing the properties of the EC material and a term of operational parameters applied to the material. It increases not only with the square of the EC coefficient ($\Phi \propto [\Delta T_{\text{EC}}/\Delta E]^2$), but also with increasing EC efficiency ($\Phi \propto c\Delta T_{\text{EC}}/\varepsilon \varepsilon_0 E^2 tan\delta$), increasing *COP* of the EC effect ($\Phi \propto \Delta T_{\text{EC}}/T$) (the latter two values were proposed separately as EC figures of merit in Refs. [49, 52], respectively), and increasing heat transfer rate ($\Phi \propto \kappa/d^2$). The larger the *FOM*, the better the cooling performance will be. For an ideal refrigerant, *FOM* becomes infinite: $FOM \rightarrow \infty$.

4.2. Best performing EC materials

The most studied and best performing EC materials are currently polyvinylidene fluoride (-CH$_2$-CF$_2$-)$_n$ terpolymers (P(VDF-TrFE-CFE)) and irradiated copolymers (P(VDF-TrFE)) as well as solid solutions of lead magnesium niobate and lead titanate ((1-x)PMN-xPT) [2]. Moreover, lead-free perovskite relaxors BaZr$_x$Ti$_{1-x}$O$_3$ (BZT) provide a ΔT_{EC} value over a broad temperature range sufficient for practical cooling applications [51]. Here, data are available solely for comparably low electric fields (up to 14.5 MV/m). Recently, a large ΔT_{EC} of 45 K was obtained for Pb$_{0.88}$La$_{0.08}$Zr$_{0.65}$Ti$_{0.3}$5O$_3$ thin films on a Pt/TiO$_2$/SiO$_2$/Si substrate at an electric field of 125 V/μm [26].

The general requirements to an EC refrigerant are:

- large and reversible polarization change,

- suitable temperature range of high EC response,

- slim or absent *P-E* hysteresis (coercive field *Ec* => 0),

- small specific heat and large thermal conductivity for fast heat transfer and

- large resistivity, i.e. small Joule heating.

Table 2 compares material characteristics [2, 5, 6, 8, 26, 51, 53], the materials efficiency Φ_{mat}, Eq. (22), and the figure of merit, Eq. (25), of promising EC refrigerants. For comparison, a thickness of 100 μm was chosen. To account for the field dependence of the dielectric permittivity ε was estimated by averaging in the given electric field region. The values of Φ_{mat} exceed significantly the ones known for Brayton engines (0.6–0.8). The only exception is the MLC due to its comparable low value of ΔT_{EC}. MLCs are still not optimized for EC application. The actual *FOM* depends on how much of the potential δT will be really used and on the field dependence of ε. The latter problem is absent in ferroelectric polymers.

4.3. Cooling power of an ideal EC element

The cooling power of an ideal EC element is given by $\dot{q} = C_{\text{EC}}\Delta T/\tau_c$, where C_{EC} is its heat capacity and $\Delta T* = \Delta T_{\text{EC}} - (T_l - T_s)$ is the temperature difference of the heat transfer steps. When the cycle time τ_c is associated by a constant factor m with the thermal time constant $\tau_{RC} = R_{th}C_{\text{EC}}$ of the EC element, the heat capacity cancels out. Consequently, $\dot{q}$ is determined

Refrigerant	T, K	ΔT_{EC}, K	ΔE, V/μm	c, MJ/m^{3}K	ε	κ, W/mK	δT, K	tanδ	Φ_{mat}	FOM, mW/cm^3
P(VDF)-based polymers	305	20	200	2.7	60	0.2	50	0.15	0.941	1.111
BaTiO$_3$	400	1.5	1	4.2	5000	2.6	5	0.05	0.9996	13.875
BaTiO$_3$	295	0.5	30	2.5	500	2.6	60	0.07	0.554	0.119
BaZr$_{0.2}$Ti$_{0.8}$O$_3$	310	4.5	15	3.4	800	2.6	30	0.05	0.994	21.739
0.7PMN-0.3PT	420	2.5	10	2.8	6000	1.5	100	0.08	0.949	1.765
0.9PMN-0.1PT	350	5	90	3	1250	1.3	100	0.1	0.986	0.311
PLZT8/65/35	385	2.5	10	3	5000	2.3	80	0.1	0.991	1.320
PLZT8/65/35	318	40	120	3	1000	2.3	80	0.07	0.963	20.295

Table 2. Material characteristics, the materials efficiency Φ_{mat} and the figure of merit selected EC refrigerants.

by the ratio of ΔT^* to the total thermal resistance R_{th} of the device. Taking into account that there are two heat transfer steps (heat absorption and heat rejection) with equal time constants and equal heat fluxes within both steps, the average cooling power per cycle yields [44]

$$\langle \dot{q} \rangle \approx \frac{\Delta T^* [1 - \exp(-m)]}{2mR_{th}}, \tag{26}$$

where $R''_{th} = A \cdot R_{th}$ is the area-specific thermal resistance given in m^2/KW. For thermal time constants with $m > 2$ (two isothermal steps at least with a duration τ_{RC}), the EC material's temperature decays to almost the steady-state value. Here, the cooling power increases linearly with frequency f. At smaller values of m, a temperature offset appears decreasing the effective ΔT^*. The maximum specific cooling power is obtained at a value of $m = \ln2 \approx 0.7$ yielding

$$\langle \dot{q} \rangle_{max} = \frac{0.36 \Delta T^*}{\sum_i R''_{th,i}}. \tag{27}$$

Table 3 compiles estimated specific cooling powers of hypothetical EC devices in dependence on the dominating thermal resistance of possible heat-releasing parts.

4.4. Cooling power of the refrigeration system

An EC refrigerator, i.e. a heat pump, is able to transport thermal energy against a temperature gradient from T_l to T_s where $T_l > T_s$. Here, the heat flows from the load to the EC layer and from the EC layer to the heat sink. Both are controlled by thermal connections that have to be opened and closed appropriately as the layer is heated or cooled. Heat is transferred from the load or to the heat sink either

i.   via controlled heat switches [58] as well as uncontrolled thermal rectifiers, or

ii.   by pumping a gaseous or liquid heat transfer agents through the solid refrigerant [59].

The heat switch or the heat transfer (HT) agent acts as an additional cycle-average thermal mass C_{HT} of the system. Correspondingly, the cycle time $\tau_c \sim R_{th}(C_{EC} + C_{HT})$ is increased.

Performance-limiting component	R''_{th}, m^2/KW	$\dot{q}$, W/cm^2	Reference
Thermal switch, MEMS (poly-Si-Si$_3$N$_4$)	1.67×10^{-5}	11	[54]
Thermal switch, Hg-droplet array	1.10×10^{-6}	164	[55]
Solid-liquid hybrid thermal interface	1.3×10^{-5}	13.9	[56]
Liquid-droplet -mediated interface	$6.7–3.2 \times 10^{-5}$	2.7–5.6	[56]
MLC, Ni-electrode	1.76×10^{-5}	10	[17]
MLC, Ag-electrode	3.86×10^{-6}	47	[17]
Liquid hexane flow	(calc.) 1.4×10^{-4}	~1	[57]
	10^{-3} (exp.)	0.36	

$\Delta T^* = 5$ K, $m = \ln 2$.

Table 3. Specific cooling power of EC devices in dependence on the dominating thermal resistance.

Usually, $C_{HT} > C_{EC}$, i.e. the cycle time is primarily determined by C_{HT}. Thus, the response times of the heat switches or the gas/liquid delivery systems limit significantly the cycle time of EC refrigerators. The thermal time constants of releasable solid-solid, liquid-solid and solid-liquid (hybrid)-solid contacts are 350, 135 and 75 ms, respectively [56]. In an AER, a secondary heat transfer agent (gas or fluid) is used to transfer heat from the cold to the hot end of the regenerator. The heat transfer agent pumped through the EC material substantially enhances the heat flow and, thus, increases the specific cooling power as well as the device efficiency. Here, the Biot number $Bi = d/(\kappa \cdot R''_{th,b})$, characterizing the ratio of the thermal resistances of the EC material volume and the boundaries, will be small for thicknesses d below 100 μm. Assuming a uniform heat flux across the interface, a height of a very long rectangular duct of 0.5 mm and a thermal conductivity of the heat transfer agent of 0.15 W/mK (silicon oil), the corresponding heat transfer coefficient $h = 1/R''_{th,b}$ yields a value of $h \approx 1250$ W/m^{2}K. At $Bi < 0.1$, the temperature of the EC element during heat transfer remains nearly constant, enabling a lumped system approximation [60]. The time constant amounts then to $\tau_i = c \cdot d/h$. It is in the order of the response time of piezoelectric valves for gas or liquid supply amounting to a few milliseconds [61]. **Table 4** compiles the time constants of hypothetical thermal interfaces and the corresponding operational frequency limits. Note that oxide thermal rectifiers made of two oxides with different thermal conductivities [62] possess a thermal contrast of $K = 1.43$ which is still too low for EC applications.

Thermal switch	τ, ms	f_{max}, Hz
Al-Si solid-solid contact	350[1]	0.5
Liquid-droplet-mediated interface	135[1]	1.2
Solid-liquid hybrid thermal interface	75[1]	2.2
Active EC regenerator	~10[2]	17

[1]Ref. [56].
[2]Calculated for $d = 5$ μm.

Table 4. Time constants of thermal interfaces and the associated frequency limit of EC devices.

Currently, the operational frequency of EC refrigerators is limited to about 10 Hz providing cooling powers of a few W/cm^2.

5. Device prototypes

EC refrigerator based on $SrTiO_3$ was initially proposed for cryogenic application, particularly in the 4–15 K temperature range [13, 63]. In a completely solid-state EC device, the electric field and magnetothermal heat switches were cycled in a proper time sequence [63]. However, no cooling power and device efficiency were reported.

For switching from a heat-conducting to a heat-insulating state near room temperature, EC elements are placed between a pair of thermoelectric elements (Peltier elements), serving as heat switch [58]. The first switch is in thermal contact with the heat sink and the second one with the load. During the adiabatic steps, both heat switches are turned off. After the EC material was adiabatically polarized (heated), the first heat switch is turned on, transferring heat from the EC element to the heat sink. The second heat switch stays turned off. After adiabatic depolarization (cooling), the second heat switch becomes active and heat is transferred from the load to the EC element. The first heat switch stays turned off. A device prototype in this configuration using Peltier elements in the passive mode was characterized in Ref. [64]. The thermal contact conductance of Peltier elements was about 1000 W/m^2K, i.e. they do not provide an advantage compared to laminar liquid flow of a heat transfer agent [57].

For EC micro-refrigerators, heat switches were fabricated by micro-electromechanic systems (MEMS) technology [43, 46, 65]. For fast heat exchange, laterally interdigitated electrodes were considered in Ref. [46]. The weak point of such a design is the comparably high thermal resistance at the interfaces to the load and the heat sink (cf. **Table 3**).

Liquid crystals were proposed as prospective heat switches [66, 67]. The operation of a thin film EC refrigerator comprising such liquid crystal heat switches was theoretically investigated in Ref. [48]. Although a thermal contrast of up to about 25 was reported for liquid crystals [68], no devices were realized yet.

A fluid-based approach uses electrohydrodynamic (EHD) flows in thin films of dielectric fluids [69]. In this case, the thermal contrast $K = 4.7 \pm 1.1$ yields a relative efficiency $\Phi_{switch} = 0.18$, which is still too low for practical application.

Table 5 compiles the parameters of EC refrigerators where the transport of thermal energy from the cold to the hot side of the system is carried out by means of heat switches. The tables illustrate that commercial multi-layer capacitors described above are an attractive EC component in proof-of-concept refrigerator prototypes. MLCs are extremely reliable. They combine a suitable thermal mass with an operating voltage in the order of 100 V as well as with the high dielectric strength obtained in thin layers (typically <10 μm) [70]. MLCs can be stacked in series to achieve a higher T_{span}. Moreover, MLC arrays can be operated between a common heat source and sink to increase cooling power.

Refrigerant	Heat switch	T, K	E, MV/m	ΔT_{EC}, °C	f, Hz	$\dot{q}$, W/cm^2	Φ	Ref.
SrTiO$_3$	Magnetothermal	10	2	0.3				[63]
n/a	Electrostatic MEMS-actuator	313	–	10		3–6	0.32	[46]
BaTiO$_3$ (MLC)	Electrostatic actuator with liquid thermal interface	300	40	0.5[1]	0.22			[43]
0.7PMN-0.3PT	Passive Peltier element	348	1.2	2.0[1]	0.42	0.035[2]		[64]
BaTiO$_3$ (MLC)	MEMS-shape Si with liquid lubricant	300	27.7	0.5[1]	0.33	0.036	0.46[2,3]	[65]
n/a	Liquid crystal		100	10		5.7[2]	0.18[2,3]	[48]
						≤150[2]	≤0.44[2,3]	
BaTiO$_3$ (MLC)	Hydrofluoroethers	298	~50	0.6[1]	0.25		0.14[2,3]	[69]

[1]Experimental value.
[2]Our estimate.
[3]Calculated using Eq. (18).

Table 5. Characteristics of EC refrigerators comprising heat switches.

A compromise between low thermal interface resistance and a quick heat transfer is a regenerator system, i.e. a heat exchanger where the heat is intermittently stored in a thermal storage medium. In the 1980s, EC cooling near 300 K was demonstrated at an operating frequency of f = 0.4 Hz using a regenerator of helium or liquid pentane that flowed back and forth between 0.3-mm-thick PbSc$_{0.5}$Ta$_{0.5}$O$_3$ plates [57, 59, 71]. The plates were rendered alternately hot and cold by electrically cycling the phase transition. The cooling power was still low at about 7.7 kg/W. Prototypes with up to 750 plates were built. In order to maintain a high temperature span in a wide temperature range, a cascade concept was realized exploiting the shift of the temperature of maximum EC activity of ceramics tailored by different sintering temperatures. A 10-fold cascade provided a temperature span of 10 K. The same operational principle can be realized using micro-electromechanical systems technology [72]. Here, the heat transfer liquid (Galden HT-70) is pumped back and forth by two diaphragm actuators, which are driven electrostatically. A small-scale EC cooling device based on an active EC regenerator with silicon oil or water as heat transfer fluids is described in Ref. [42].

The heat regeneration process is commonly used to increase the temperature span in cooling devices. Experimentally obtained regeneration factors (ratio between the temperature span established across the device and ΔT_{EC}) are ca. 2 [71] and ca. 3.7 [42], respectively. Simulations predict an improvement by a factor of 5–6 [71] and, by optimizing also the heat transfer agent, up to a factor of 10 [42]. Thus, temperature spans of up to 20 K seem to be technically possible.

Regeneration can be realized also by heat exchange directly between EC elements that are rotating in opposite directions with different applied fields. A corresponding rotary EC refrigerator is described in Ref. [47]. It consists of stacked EC rings where each EC ring is composed of N_s (for example, N_s = 16) thermally separated EC elements. The EC rings rotate coaxially with the same rotary speed, but the rotation directions are opposite between neighbouring rings. Every

two neighbouring EC rings are directly contacted to facilitate the heat exchange with each other. Heat exchangers with high thermal conductivity are placed at the circumference at opposite sides of the device to absorb or reject heat. Simulation results showed a cooling power density of 37 W/cm^3 for a T_{span} of 20 K for a cooling device made of P(VDF-TrFE-CFE) terpolymer.

The electrocaloric oscillatory refrigeration device (ECOR) adapts a concept known from thermoacoustic cooling [28, 73]. It consists of an EC element and a solid-state regenerator. The length of the EC module is slightly shorter than that of the regenerator, so that the EC module can move back and forth on the regenerator. Thereby, a temperature gradient is established within both and heat is transported from one side to the other. The solid-state regenerator

Refrigerant	Configuration	T, K	E, MV/m	ΔT_{EC}, °C	f, Hz	$\dot{q}$, W/cm²	Φ	Ref.
PST	AER		1.5	0.9	4	0.05		[59]
			3[1]	1.5[1]	5			
		260–280	6	3		0.36		[57]
		280–300	1.5	0.9			0.42	[71]
P(VDF–TrFE–CFE) 59.2/33.6/7.2	Fluid-based micro-scale refrigerator	300	150	16	10	3	0.31	
			50		10	0.173		[72]
			50		20	2		
0.9PMN-0.1PT	Small scale AER		115	1.5	1.25			[42]
			87	1.25				
		300	57		0.75			
			50	0.9[1]	0.75			
			25	0.6[1]				
Ba(Zr,Ti)O$_3$ (MLC)			20	0.54[1]	0.02	0.006[1]		[73]
		298			5	0.083		
					0.02			
					5			
n/a	EC refrigerator with internal regenerator	323	150	14.6	1.25	~4	0.57	[47]
P(VDF-TrFE) 68/32 (irrad.)	Chip scale EC oscillatory refrigerator (ECOR)		50		0.5			[74]
			80	2.2[1]	0.5			
			100		0.5			
		308	100		1			
			100		3			
			150		0.5			
			160	21[1]	10	5.4	0.5	[28]

[1]Experimental value.

Table 6. Characteristics of EC refrigerators using regeneration.

might possess an anisotropic thermal conductivity highly reducing heat conduction losses. A 1 cm long device can provide a cooling density of 9 W/cm^3. The weak point of this design is the friction during the relative motion between EC element and regenerator.

Table 6 illustrates the characteristics of EC refrigerators using regeneration. Although the cooling power of experimental prototypes is still very low, modelling based on experimental results predicts cooling powers of a few W/cm^2.

6. Conclusions

EC cooling is an environment-friendly caloric energy conversion technology. Cooling power densities of a few W/cm^2 and temperature spans in the order of 20 K (in regeneration systems) are achievable at a cycle time of 100 ms. Currently, EC cooling does not represent an alternative for the full replacement of vapour compression. It can be assumed that it will rather penetrate niche markets in the future such as small, compact, local and all-solid-state refrigerators. Although the reverse Brayton thermodynamic cycle is actually the most suitable for practical implementation, further research on more efficient cycles is required. EC cooling processes possess a large materials efficiency and are thermodynamically reversible. At present, the bottleneck of EC refrigerators is the heat transfer process needed to absorb heat from the load and reject it to the heat sink. Most attractive for applications are all-solid-state devices including Peltier elements as thermal switches and active electrocaloric regenerators using a liquid heat transfer agent.

Author details

Gunnar Suchaneck[1]*, Oleg Pakhomov[2] and Gerald Gerlach[1]

*Address all correspondence to: gunnar.suchaneck@tu-dresden.de

1 TU Dresden, Solid State Electronics Laboratory, Dresden, Germany

2 ITMO National Research University (ITMO University), St. Petersburg, Russia

References

[1] Calm JM. Comparative efficiencies and implications for greenhouse gas emissions of chiller refrigerants. International Journal of Refrigeration [Revue Internationale Du Froid]. 2006;**29** (5):833–841. DOI: 10.1016/j.ijrefrig.2005.08.017

[2] Valant M. Electrocaloric materials for future solid-state refrigeration technologies. Progress in Materials Science. 2012;**57**(6):980–1009. DOI: 10.1016/j.pmatsci.2012.02.001

[3] Ožbolt M, Kitanovski A, Tušek J, Poredoš A. Electrocaloric vs. magnetocaloric energy conversion. International Journal of Refrigeration [Revue Internationale Du Froid]. 2014;**37** (January 2014):16–27. DOI: 10.1016/j.ijrefrig.2013.07.001

[4] Birks E, Dunce M, Sternberg A. High electrocaloric effect in ferroelectrics. Ferroelectrics. 2010;**400**(1):336–343. DOI: 10.1080/00150193.2010.505854

[5] Alpay PS, Mantese J, Trolier-McKinstry S, Zhang Q, Whatemore RW. Next generation electrocaloric and pyroelectric materials for solid-state electrothermal energy interconversion. MRS Bulletin. 2014;**39**(12):1099–1109. DOI: 10.1557/mrs.2014.256

[6] Ožbolt M, Kitanovski A, Tušek J, Poredoš A. Electrocaloric refrigeration: Thermodynamics, state of the art and future perspectives. International Journal of Refrigeration [Revue Internationale Du Froid]. 2014;**40**(April 2014):174–188. DOI: 10.1016/j.ijrefrig.2013.11.007

[7] Qian S, Nasuta D, Rhoads A, Wang Y, Geng Y, Hwang Y, et al. Not-in-kind cooling technologies: A quantitative comparision of refrigerants and system performance. International Journal of Refrigeration [Revue Internationale Du Froid]. 2016;**62**:177–192. DOI:10. 1016/j.ijrefrig.2015.10.019

[8] Correia T, Zhang Q, editors. Electrocaloric Materials: New Generation of Coolers. Berlin-Heidelberg: Springer; 2014. p. 253. DOI: 10.1007/978-3-642-40264-7

[9] Thomson W. On the thermoelastic, thermomagnetic and pyroelectric properties of matter. Philosophical Magazine Series 5. 1878;**5**(28):4–27. DOI: 10.1080/14786447808639378

[10] Kobeko P, Kurtschatov J. Dielektrische Eigenschaften der Seignettesalzkristalle. Zeitschrift für Physik. 1930;**66**(3):192–205. DOI: 10.1007/BF01392900

[11] Baumgartner H. Elektrische Sättigungserscheinungen und elektrokalorischer Effekt von Kaliumphosphat KH_2PO_4. Helvetica Physica Acta. 1950;**23**(6/7):651–696. DOI: 10.5169/ seals-112128

[12] Roberts S. Adiabatic study of 128°C transition in barium titanate. Physical Review. 1952;**85**(5):925–926. DOI: 10.1103/PhysRev.85.925.2

[13] Gränicher H. Induzierte Ferroelektrizität von $SrTiO_3$ bei sehr tiefen Temperaturen und über die Kälteerzeugung durch adiabatische Entpolarisierung. Helvetica Physica Acta. 1956;**29**(3):210–212

[14] Tuttle BA, Payne DA. The effect of microstructure on the electrocaloric properties of Pb(Zr, Sn,Ti)O_3 ceramics. Ferroelectrics. 1981;**37**(1):603–606. DOI: 10.1080/00150198108223496

[15] Mischenko AS, Zhang Q, Scott JF, Whatmore RW, Mathur ND. Giant electrocaloric effect in thin film $PbZr_{0.95}Ti_{0.05}O_3$. Science. 2006;**311**(5765):1270–1271. DOI: 10.1126/science.1123811

[16] Bai Y, Zheng G-P, Ding K, Qiao L, Shi S-Q, Guo D. The giant electrocaloric effect and high effective cooling power near room temperature for $BaTiO_3$ thick film. Journal of Applied Physics. 2011;**110**(9):094103. DOI: 10.1063/1.3658251

[17] Kar-Narayan S, Mathur ND. Direct and electrocaloric measurements using multilayer capacitors. Journal of Physics D-Applied Physics. 2010;**43**(3):032002. DOI: 10.1088/0022-3727/43/3/032002

[18] Herbert JM. Thin ceramic dielectrics combined with nickel electrodes. Proceedings of the Institution of Electrical Engineers. 1965;**112**(7):1474–1477. DOI: 10.1049/piee.1965.0237

[19] Sakabe Y, Minai K, Wakino K. High-dielectric constant ceramics for base metal mono-lithic capacitors. Japanese Journal of Applied Physics. 1981;**20**(Suppl. 20-4):147–150. DOI: 10.7567/JJAPS.20S4.147

[20] Kishi H, Mizuno Y, Chazono H. Base-metal electrode-multilayer ceramic capacitors: Past, present and future perspectives. Japanese Journal of Applied Physics. 2003;**42**(Part 1, Number 1):1–15. DOI: 10.1143/JJAP.42.1

[21] Lines ME, Glass AM. Principles and Application of Ferroelectrics and Related Materials. 1st ed. Oxford: Clarendon Press; 1977. p. 148. ISBN: 0486648710

[22] Suchaneck G, Gerlach G. Electrocaloric cooling based on relaxor ferroelectrics. Phase Transitions. 2015;**88**(3):333–341. DOI: 10.1080/01411594.2014.989225

[23] Suchaneck G, Gerlach G. Requirements to (Ba,Ca)(Zr,Ti)O$_3$ electrocaloric materials. In: 2013 Joint IEEE International Symposium on Application of Ferroelectrics and Workshop on Piezoresponse Force Microscopy (ISAF/PFM); 21–25 July 2013; Prague: IEEE; 2013. pp. 244–247. DOI: 10.1109/ISAF.2013.6748680

[24] Karchevskii AI. Electrocaloric effect in polycrystalline barium titanate. Soviet Physics Solid State. 1962;**3**:2249–2254

[25] Bai Y, Zheng G-P, Shi S-Q. Kinetic electrocaloric effect and giant net cooling of lead-free ferroelectric refrigerants. Journal of Applied Physics. 2010;**108**(10):104102. DOI: 10.1063/1.3511342

[26] Lu SG, Rožič B, Zhang QM, Kutnjak Z, Li X, Furman E, et al. Organic and inorganic relaxor ferroelectrics with giant electrocaloric effect. Applied Physics Letters. 2010;**97**(16): 162904. DOI: 10.1063/1.3501975

[27] Novak N, Pirc R, Kutnjak Z. Impact of critical point on piezoelectric and electrocaloric response in barium titanate. Physical Review B. 2013;**87**(10):104102. DOI: 10.1103/PhysRevB.87.104102

[28] Li X, Gu H, Qian X, Zhang Q. Compact cooling devices based on giant electrocaloric effect. In: 13th IEEE Intersociety Conference on Thermal and Thermomechanical Phe-nomena in Electronic Systems (ITherm); 30 May–1 June 2012; San Diego, CA (USA), IEEE; 2012. pp. 934–937. DOI: 10.1109/ITHERM.2012.6231525

[29] Clapeyron MC. Mémoire sur la puissance motrice de la chaleur. J. de l´École polytechnique. 1834;**23**:153–190. ark: /12148/bpt6k4336791/f157

[30] Neese B, Chu B, Lu S-G, Wang Y, Furman E, Zhang QM. Large electrocaloric effect in ferroelectric polymers near room temperature. Science. 2008;**321**(5890):821–823. DOI: 10.1126/science.1159655

[31] Peräntie J, Hagberg J, Uusimäki A, Jantunen H. Field induced thermal response and irreversible phase transition enthalpy change in $Pb(Mg_{1/3}Nb_{2/3})O_3$-$PbTiO_3$. Applied Physics Letters. 2009;**94**(10):102903. DOI: 10.1063/1.3098067

[32] Peräntie J, Tailor HN, Hagberg J, Ye Z-G. Electrocaloric properties in relaxor ferroelectric (1-x)$Pb(Mg_{1/3}Nb_{2/3})O_3$-x$PbTiO_3$ system. Journal of Applied Physics. 2013;**114**(17):174105. DOI: 10.1063/1.4829012

[33] Mohammadi S, Khodayari A, Ahmadi A. Electrocaloric response of ferroelectric material applicable as electrothermal transducer. Advances in Materials Science and Engineering. **2013**;2013:858656. DOI: 10.1155/2013/858656

[34] Kutnjak Z, Blinc R, Ishibashi Y. Electric field induced critical points and polarization rotation in relaxor ferroelectrics. Physical Review B. 2007;**76**(10):104102. DOI: 10.1103/PhysRevB.76.104102

[35] Pirc R, Kutnjak Z, Blinc R, Zhang QM. Upper bounds on the electrocaloric effect in polar solids. Applied Physics Letters. 2011;**98**(2):021909. DOI: 10.1063/1.3543628

[36] Suchaneck G, Gerlach G, Deyneka A, Jastrabik L, Davitadze ST, Strukov BA. Phase transitions of self-polarized PZT thin films. MRS Proceedings. 2002;718:718-D8.4. DOI: 10.1557/PROC-718-D8.4

[37] Suchaneck G, Gerlach G. Lead-free relaxor ferroelectrics for electrocaloric cooling. Materials Today: Proceedings. 2016;**3**(2):622–631. DOI: 10.1016/j.matpr.2016.01.100

[38] McPherson J, Kim J-Y, Shanware A, Mogul H. Thermochemical description of dielectric breakdown in high dielectric constant materials. Applied Physics Letters. 2003;**82**(13):2121–2123. DOI: 10.1063/1.1565180

[39] Yu Z, Ang C, Guo R, Bhalla AS. Ferroelectric-relaxor behavior of $Ba(Ti_{0.7}Zr_{0.3})O_3$ ceramics. Journal of Applied Physics. 2002;**92**(5):2655–2657. DOI: 10.1063/1.1495069

[40] He J, Chen J, Zhou Y, Wang JT. Regenerative characteristics of electrocaloric Stirling or Ericsson refrigeration cycles. Energy Conversion and Management. 2002;**43**(17):2319–2327. DOI: 10.1016/S0196-8904(01)00183-2

[41] Olsen RB, Biscoe JM, Bruno DA, Butler WF. A pyroelectric energy converter which employs regeneration. Ferroelectrics. 1981;**38**(1):975–978. DOI: 10.1080/00150198108209595

[42] Plaznik U, Kitanovski A, Rožič B, Malič B, Uršič H, Dmovšek S, et al. Bulk relaxor ferroelectric ceramics as a working body for electrocaloric cooling device. Applied Physics Letters. 2015;**106**(4):043903. DOI: 10.1063/1.4907258

[43] Jia Y, Ju YS. A solid-state refrigerator based on the electrocaloric effect. Applied Physics Letters. 2012;**100**(24):242901. DOI: 10.1063/1.4729038

[44] Suchaneck G, Gerlach G. Materials and device concepts for electrocaloric refrigeration. Physica Scripta. 2015;**90**(9):094020. DOI: 10.1088/0031-8949/90/9/094020

[45] Kirillin VA, Sytchev VV, Sheindlin AE. Engineering Thermodynamics. 1st ed. Moscow: Mir Publishers; 1976. p. 560.

[46] Ju SY. Solid-state refrigeration based on the electrocaloric effect for electronics cooling. Journal of Electronic Packaging. 2010;**132**(4):041004. DOI: 10.1115/1.4002896

[47] Gu H, Qian X-S, Ya H-J, Zhang QM. An electrocaloric refrigerator without external regenerator. Applied Physics Letters. 2014;**105**(16):162905. DOI: 10.1063/1.4898812

[48] Epstein RI, Malloy KJ. Electrocaloric devices based on thin-film heat switches. Journal of Applied Physics. 2009;**106**(6):064509. DOI: 10.1063/1.3190559

[49] Defay E, Crossley S, Kar-Narayan S, Moya X, Mathur ND. The electrocaloric efficiency of ceramic and polymer films. Advanced Materials. 2013;**25**(24):3337–3342. DOI: 10.1002/adma.201300606

[50] Gschneider Jr KA, Pecharsky VK, Tsokol AO. Recent developments in magnetocaloric materials. Reports on Progress in Physics. 2005;**68**(6):1479–1539. DOI: 10.1088/0034-4885/68/6/R04

[51] Qian X-S, Ye H-J, Zhang Y-T, Gu H, Li X, Randall CA, et al. Giant electrocaloric response over a broad temperature range in modified BaTiO$_3$ ceramics. Advanced Functional Materials. 2014;**24**(9):1300–1305. DOI: 10.1002/adfm.201302386

[52] Guzmán-Verri GG, Littlewood PB. Why is the electrocaloric effect so small in ferroelectrics? APL Materials. 2016;**4**(6):064106. DOI: 10.1063/1.4950788

[53] Suchaneck G. Upper bounds in electrocaloric cooling. In: 2016 Joint IEEE International Symposium on Application of Ferroelectrics, European Conference on Polar Dielectrics, and Piezoelectric Force Microscopy Workshop (ISAF/ECAPD/PFM); 21–25 August 2016; Darmstadt. Piscataway, NJ: IEEE; 2016. p. 4. DOI: 10.1109/ISAF.2016.7578104

[54] Cho J, Richards C, Bahr D, Jiao J, Richards R. Evaluation of contacts for a MEMS thermal switch. Journal of Micromechanics and Microengineering. 2008;**18**(10):105012. DOI: 10.1088/0960-1317/18/10/105012

[55] Song W-B, Sutton MS, Talghader JJ. Thermal contact conductance of actuated interfaces. Applied Physics Letters. 2002;**81**(7):1216–1218. DOI: 10.1063/1.1499518

[56] Jia Y, Ju YS. Solid-liquid hybrid thermal interfaces for low-contact pressure thermal switching. Journal of Heat Transfer. 2014;**136**(7):074503. DOI: 10.1115/1.4027205

[57] Sinyavsky YV, Brodyansky VM. Experimental testing of electrocaloric cooling with transparent ferroelectric ceramics as a working body. Ferroelectrics. 1992;**131**(1):321–325. DOI: 10.1080/00150199208223433

[58] Mathur N, Mishenko A., inventors; Cambridge University Technical Services, assignee. Solid state electrocaloric cooling devices and methods. World Intellectual Property Organization patent application WO 2006056809 A1; 2006 June 1.

[59] Sinyavsky YV, Pashkov ND, Gorovoy YM, Lugansky GE, Shebanov L. The optical ferroelectric ceramic as working body for electrocaloric refrigeration. Ferroelectrics. 1989;**90**(1):213–217. DOI: 10.1080/00150198908211296

[60] Bergman TL, Lavine AS, Incropera FP, DeWitt DP. Fundamentals of Heat and Mass Transfer. 7th ed. Hoboken, NJ: John Wiley & Sons Inc.; 2011. p. 1048. ISBN: 978-0470501979

[61] Rogge T, Rummler Z, Schomburg WK. Polymer micro valve with a hydraulic piezo-drive fabricated by AMANDA process. Sensors and Actuators A. 2004;**110**(1–3):206–212. DOI: 10.1016/j.sna.2003.10.056

[62] Kobayshi W, Teraoka T, Terasaki I. An oxide thermal rectifier. Applied Physics Letters. 2009;**95**(17):171905. DOI: 10.1063/1.3253712

[63] Radebaugh R, Lawless WN, Siegwarth JD, Morrow AJ. Electrocaloric refrigeration at cryogenic temperatures. Ferroelectrics. 1980;**27**(1):205–211. DOI: 10.1080/00150198008226100

[64] Chukka R, Vandrangi S, Shannigrahi S, Chen L. An electrocaloric device demonstrator for solid-state cooling. Europhysics Letters. 2013;**103**(4):47011. DOI: 10.1209/0295-5075/103/47011

[65] Wang YD, Smullin SJ, Sheridan MJ, Wang Q, Eldershaw C, Schwartz DE. A heat-switch-based electrocaloric cooler. Applied Physics Letters. 2015;**107**(13):134103. DOI: 10.1063/1.4932164

[66] Epstein RI, Malloy KJ. inventors; Epstein RI, Malloy KJ, assignee. Electrocaloric refrigerator and multilayer pyroelectric energy generator. United States patent application US20100037624 A1; 2010 February 18

[67] Epstein RI, Malloy KJ. inventors; Stc. Unm, assignee. Electrocaloric refrigerator and multilayer pyroelectric energy generator. United States patent application US20130074900 A1; 2013 March 28

[68] Carr EF. Electrohydrodynamics and the heat switch. Molecular Crystals and Liquid Crystals. 1991;**2002**(1):1–6. DOI: 10.1080/00268949108035653

[69] Hehlen MP, Mueller AH, Weisse-Bernstein NR, Epstein RI. Electrocaloric refrigerator using electrohydrodynamic flows in dielectric fluids. In: Epstein RI, Seletskiy DV, Sheik-Bahae M, editors. Proceedings of SPIE 8638, Laser Refrigeration of Solids VI. Bellingham, WA: SPIE; 2013. p. 86380D. DOI: 10.1117/12.2004009

[70] Milliken AD, Bell AJ, Scott JF. Dependence of breakdown field on dielectric (interelectrode) thickness in base-metal electroded multilayer capacitors. Applied Physics Letters. 2007;**90**(11):112910. DOI: 10.1063/1.2713780

[71] Sinyavsky YuV. Electrocaloric refrigerators: A promising alternative to current low-temperature apparatus. Chemical and Petroleum Engineering. 1995;**31**(6):295–306. DOI: 10.1007/BF01148217

[72] Guo D, Gao J, Yu Y-Y, Santhanam S, Slippey A, Fedder GK, et al. Design and modeling of a fluid-based micro-scale electrocaloric refrigeration system. International Journal of Heat and Mass Transfer. 2014;**72**(May 2014):559–564. DOI: 10.1016/j.ijheatmasstransfer.2014.01.043

[73] Sette D, Asseman A, Gérard M, Strozyk H, Faye R, Defay E. Electrocaloric cooler combining ceramic multi-layer capacitors and fluid. APL Materials. 2016;**4**(9):091101. DOI: 10.1063/1.4961954

[74] Gu H, Qian X, Li X, Craven B, Zhu W, Cheng A, et al. A chip scale electrocaloric effect based cooling device. Applied Physics Letters. 2013;**102**(12):122904. DOI: 10.1063/1.4799283